Progress In Electromagnetics Research C, Vol. 134, 143–155, 2023

Coplanar Fed Quad-Band Parasitic Patch Antenna for Ultra-Wideband Wireless Application

Anil K. Bhat[1, 2, *], Ashish Singh[1], Ramya Shetty[1], and Satheesh Rao[1]

Abstract—In this article the design of an ultra-wideband coplanar monopole antenna with a microstrip parasitic patch having a dimension of 50 mm × 50 mm using a 1 mm thick RT-Duroid substrate ($\varepsilon_r = 2.2$) is explored for wireless applications. Five different coplanar antenna designs are presented, and one of the designs is proposed for fabrication. In simulation the proposed antenna has four resonant bands, 2.043–2.133 GHz, 5.821–7.89 GHz, 10.3–12.027 GHz, and 12.783–17.802 GHz, with a cumulative bandwidth of 8.905 GHz within 1–18 GHz. The proposed antenna is fabricated, tested, and validated using Vector Network Analyzer. Fabricated antenna resonates at four different bands, 2.349–2.888 GHz, 5.767–7.926 GHz, 9.725–10.534 GHz, and 13.862–16.021 GHz with resonant peaks at 2.529 GHz, 7.116 GHz, 10.084 GHz, and 15.391 GHz frequencies, respectively. Further the antenna has a cumulative bandwidth of 5.666 GHz in 1–18 GHz band. Radiation efficiency is above 90% at the resonant band. The acquired results from simulation and measurement are in close match.

1. INTRODUCTION

Ultra-wideband (UWB) communication is a type of wireless communication that uses a large portion of the radio spectrum to transmit data over short distances. UWB communication offers high data rates, low power, low latency, high security, and can easily operate with the existing wireless communication technologies. With the release of 7.5 GHz radio spectrum from 3.1–10.6 GHz by the Federal Communication Commission (FCC) for UWB wireless communication applications, there has been a lot of interest in this channel [1]. One of the important blocks of wireless communication systems are UWB antenna. UWB antennas can transmit and receive signals over a broad frequency range, typically having bandwidth $\geq$ 500 MHz or bandwidth $\geq$ 20% as per FCC [1]. UWB antennas can be realized using various techniques such as microstrip line, electromagnetic band gap (EBG) structures, and planar inverted-F antennas, among others. Among them, microstrip patch antenna (MSPA) has many advantages like ease of design and fabrication, small size, and compatibility with microwave integrated circuits (MICs) [11, 12]. Many different types of patch antennas have been reported in literature with varying specifications and applications. UWB technology has numerous applications across various industries due to its unique characteristics. Due to their high-speed data transfer capability, UWB antennas can be used for short-range wireless communication between devices. Typical applications include wireless USB, Bluetooth, wireless High-Definition Multimedia Interface (HDMI) connections, etc. UWB antennas can be utilized in precise indoor positioning and tracking systems and can determine the location of objects or people with centimetre-level accuracy. This technology finds applications in asset tracking, personnel monitoring, and security systems. UWB antennas are suitable for radar applications due to their wide frequency coverage and ability to provide high-resolution imaging. UWB radar systems are used for target detection, localization, and imaging in areas such as automotive radar, ground penetrating radar, through-wall imaging, and object recognition. UWB

Received 18 May 2023, Accepted 22 June 2023, Scheduled 6 July 2023
* Corresponding author: Anil Kumar Bhat (anilkumarbhat@nitte.edu.in).
[1] NITTE (Deemed to be University), Department of Electronics & Communication Engineering, NMAM Institute of Technology, Nitte, Karnataka 574110, India. [2] Visvesvaraya Technological University (VTU), Belagavi, Karnataka 590018, India.

antennas are utilized in emerging technologies such as V2V and V2I communication systems enabling vehicles to communicate with each other and with roadside infrastructure, improving safety, traffic management, and autonomous driving capabilities [2].

In this article a detailed design of a coplanar fed UWB antenna, having an overall dimension of 50 mm × 50 mm using a 1 mm thick RT Duroid substrate (RT5880) with dielectric constant 2.2, is proposed. The antenna is designed for wireless applications using the 1–18 GHz spectrum.

2. ANTENNA DESIGN

The antenna is intended for wireless applications in the frequency band of 1–18 GHz. In this frequency range, the bands of interest are 2.4 GHz ISM Band (2.401–2.495 GHz), 5 GHz ISM Band (5.175–5.85 GHz), and 6 GHz Wi-Fi Band (5.915–7.135 GHz).

For an MSPA, the smaller the dielectric constant is, the better the efficiency and bandwidth are [8], hence, RT Duroid 5880 ($\varepsilon_r = 2.2$), was chosen as the substrate for the design. As the maximum frequency of interest was 7.2 GHz, the height of the substrate was chosen using Equation (1) [8, 9]. The calculated value for maximum substrate height is 1.27 mm, so a 1 mm thick substrate was chosen in the design.

$$h \leq \frac{0.3\lambda_0}{2\pi\sqrt{\varepsilon_r}} \tag{1}$$

A coplanar waveguide (CPW) feed is chosen for the design as it is simple to fabricate, enables surface mount options for active and passive devices, and has reduced radiation losses and lower cross talk effects [5, 8, 9].

The radius of the circular patch with a centre frequency of 2.4 GHz is calculated using Equations (2), (3), given in [8, 9]. The calculated radius for the circular patch is 22 mm. The designed antenna is shown in Fig. 1(a).

$$a_e \leq \frac{1.84118\lambda_0}{2\pi\sqrt{\varepsilon_e}} \tag{2}$$

$$a = a_e - 4 \times \frac{h}{\sqrt{\varepsilon_r}} \tag{3}$$

Antenna_1, of Fig. 1(a) has resonant peaks at 7.1447 GHz (12% BW, total efficiency of 86.5%, and maximum gain of 4.799) and 16.492 GHz (15% BW, total efficiency of 97.4%, and maximum gain of 8.051). To improve the bandwidth, a circular defect was created in the parasitic patch as shown in Fig. 1(b). This second structure with parasitic annular ring, termed Antenna_2, has resonant peaks at 2.586 GHz (7.98% BW, 48.46% efficiency, maximum gain of −0.881), 7.188 GHz (20.7% BW, 98.19% efficiency, maximum gain of 5.69) and at 13.107 GHz (> 50% BW, 93.89% efficiency, maximum gain of 7.04) [6, 7]. This design can be used for frequencies above 10.8 GHz. To improve the gain, a square patch of size 22 mm was added at the centre of annular ring [3, 4]. The size of the patch was calculated using Equations (4) and (5) which are the general equations for rectangular microstrip antenna (MSA) in fundamental TM_{10} mode as given in [8, 9].

$$f_o = \frac{C}{2L\sqrt{\varepsilon_e}} \tag{4}$$

$$\varepsilon_e = \frac{(\varepsilon_r + 1)}{2} + \frac{(\varepsilon_r - 1)}{2}\left[1 + \frac{10h}{W}\right]^{-1/2} \tag{5}$$

The structure of Antenna_3 is shown in Fig. 1(c). With the addition of the square patch, Antenna_3 resonated at two frequencies, 7.134 GHz (21.8% BW, 96.2% efficiency, maximum gain of 5.965) and 13.411 GHz (BW > 37%, 77.8% efficiency, maximum gain of 5.557). Another square patch of same dimension but rotated by 45° angle was added to make the central structure appear like a star as shown in Fig. 1(d) [Antenna_4]. The resonant peaks are at 7.299 GHz, 12.849 GHz, and 17.73 GHz.

An annular ring defect was introduced in the star, and the new antenna structure, Antenna_5, is shown in Fig. 1(e). The new structure has resonant peaks at 7.3139 GHz (21.5% BW, 88.79% efficiency,

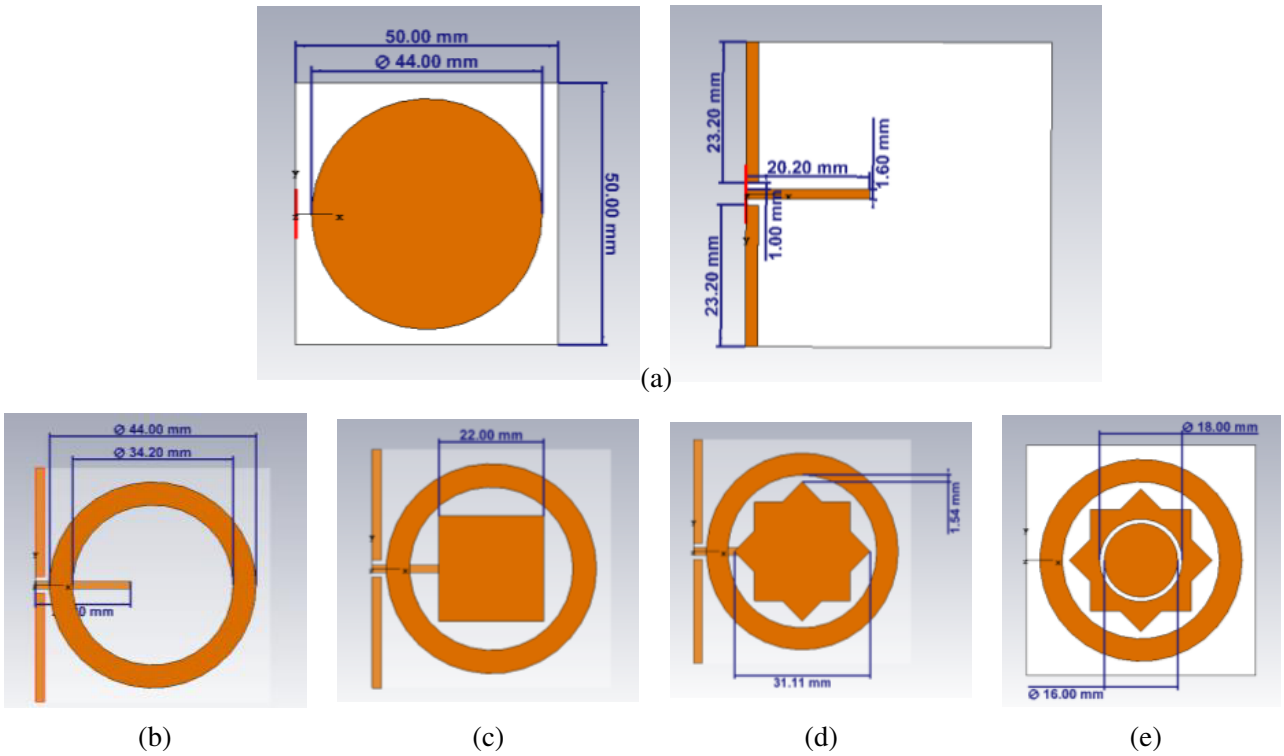

Figure 1. Intermediate structures of the proposed antenna: (a) Top and bottom view of circular patch designed to resonate at 2.4 GHz (Antenna_1), (b) annular ring parasitic patch (Antenna_2), (c) addition of square patch to improve gain (Antenna_3), (d) addition of copper area by using a 45° rotated square forming a star structure (Antenna_4), (e) addition of slot to improve bandwidth (Antenna_5).

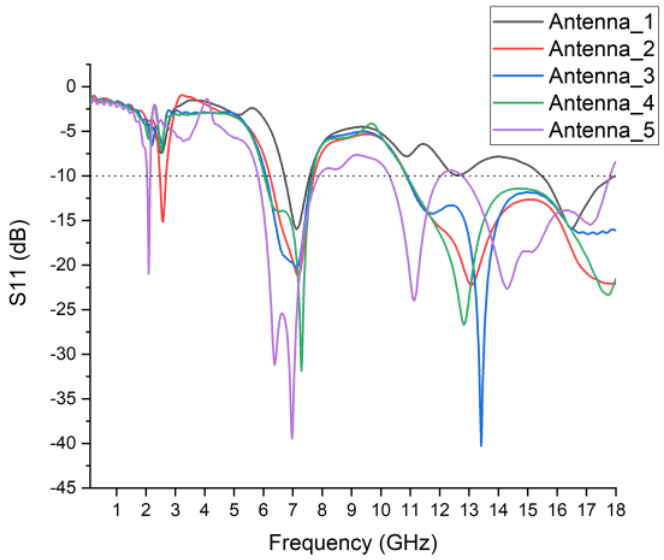

Figure 2. Simulated results for S_{11} for coplanar fed MSPA structures shown in Fig. 1.

maximum gain of 6.05) and at 11.861 GHz, 13.072 GHz, and 17.679 GHz (> 8 GHz BW including all three peaks). This antenna structure has minimum efficiency of 94% and maximum gain above 6.156 and hence is a promising structure for UWB applications. The simulated results for S_{11} for the different antenna structures are shown in Fig. 2.

Table 1. Comparison of parameters of the simulated and measured values for the proposed antenna.

Antenna Structure		Antenna Simulation Parameters				
	Centre Frequency (GHz)	Lower Cut-off (GHz)	Higher Cut-off (GHz)	BW	Max Gain (dB)	Efficiency (dB)
Antenna_1	7.1477	6.7164	7.5791	12.07%	4.7997	−1.2558
	16.7175	15.479	17.956	14.82%	8.0512	−0.2344
Antenna_2	2.5811	2.478	2.6843	7.99%	−0.8815	−6.2906
	6.9714	6.2207	7.7221	21.54%	5.6999	−0.1586
	14.441	10.882	18*	49.29%	7.0414	−0.5475
Antenna_3	6.8601	6.0824	7.6379	22.67%	5.9650	−0.3408
	14.4425	10.885	18*	49.26%	5.5577	−1.0881
Antenna_4	6.8443	6.0263	7.6623	23.90%	6.3058	−0.3989
	14.4245	10.849	18*	49.58%	6.8375	−0.3759
Antenna_5	6.8351	6.0088	7.6615	24.18%	6.1560	−0.3873
	14.4255	10.851	18*	49.56%	7.8037	−0.1227

* Simulation was done from 0.01 MHz to 18 GHz only

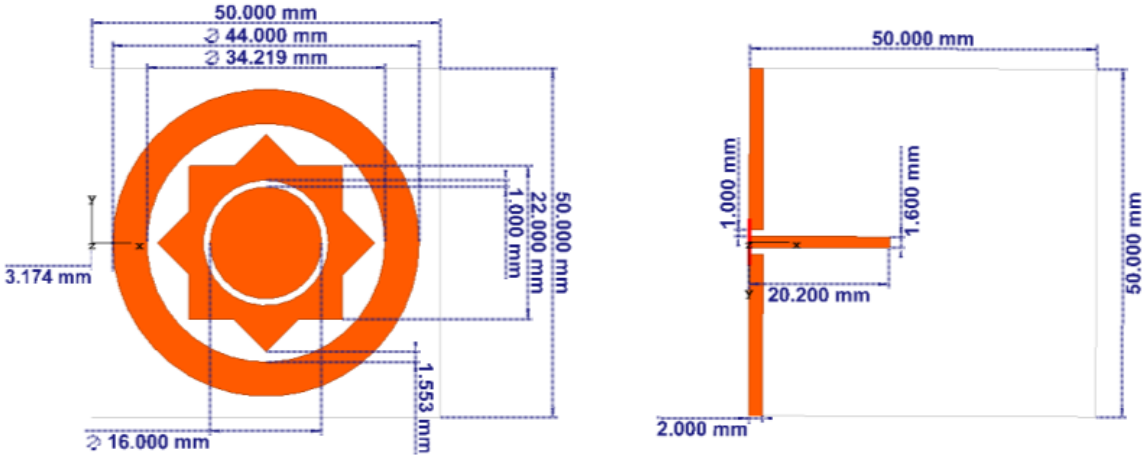

Figure 3. Top and bottom side view of proposed antenna for UWB applications.

The simulation results for the antenna structures of Fig. 1 is tabulated in Table 1. All the presented structures have UWB properties and can be considered for UWB applications. Due to novelty of the structure, the antenna design of Figure 1(e) was chosen for further optimization. A parametric analysis was done by varying the dimensions of the gaps, and the optimum structure with the best results for S_{11} shown in Fig. 3 was considered for fabrication.

The proposed antenna has radiating dimension of $(50\times50\times1)$ mm^3 and uses an RT Duroid substrate with $\varepsilon_r = 2.2$. Three parasitic patches are used, an annular ring with outer radius of 22 mm and ring thickness of 4.8905 mm, a star structure constructed using two squares of 22 mm side, and an annular ring defect of 1 mm thick and outer radius of 8 mm. The parasitic patch has a maximum dimension of (44×44) mm^2 with a coplanar fed microstrip line of dimension (20.2×1.6) mm^2. The proposed antenna is shown in Fig. 3, and its simulated S_{11} results are shown in Fig. 4. The proposed structure has four resonant bands and shows UWB characteristics. The antenna was fabricated, and its top and bottom views are shown in Fig. 5.

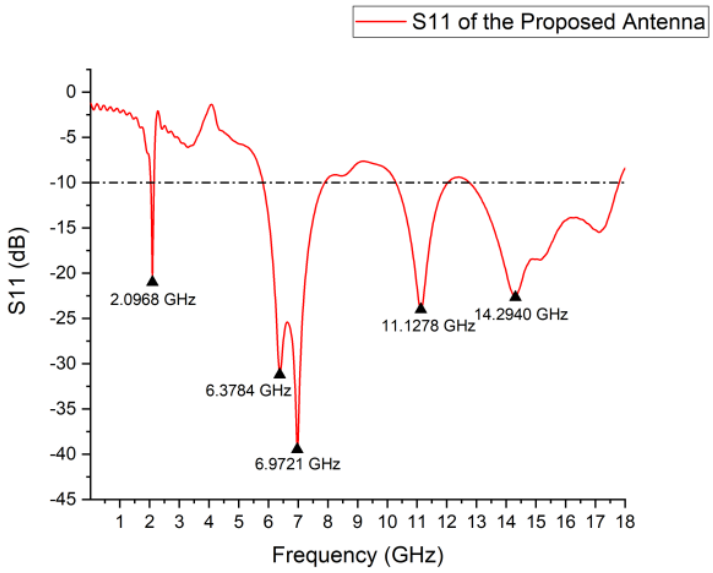

Figure 4. Simulated results for S_{11} for the proposed antenna.

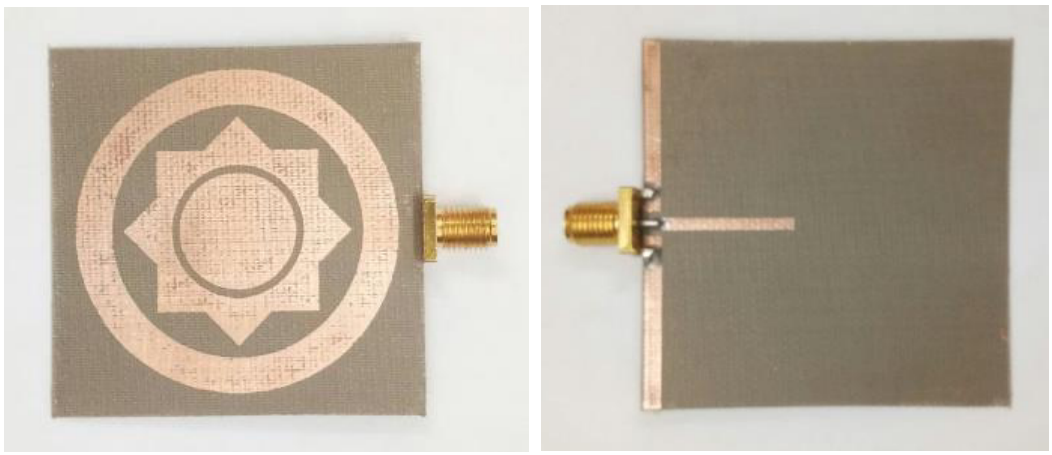

Figure 5. Fabricated antenna top and bottom view.

3. RESULTS AND DISCUSSION

The proposed antenna was fabricated, and the reflection coefficient has been measured using Agilent N5247A. The reflection coefficient measurement setup and the measurements are given in Fig. 6.

As seen from the reflection coefficient measurements graph in Fig. 6, there are four resonant bands. The first band is from 2.349 GHz to 2.888 GHz with the centre frequency at 2.6185 GHz. The bandwidth available is 539 MHz (20.58%). The second band is centred at 6.8465 GHz spanning 5.767 GHz to 7.926 GHz (31.53% BW). The third band spans from 9.725 GHz to 10.534 GHz providing 809 MHz bandwidth centred at 10.1295 GHz which amounts to 7.98% BW. The fourth band has a bandwidth of 2.159 GHz spanning 13.862 GHz to 16.021 GHz with the centre frequency at 14.9415 GHz (14.45% BW). The simulated and measured parameters for the antenna of Fig. 5 are tabulated in Table 2. Fig. 7 shows the plot of simulated and measured values of S_{11}.

As can be seen from Table 2 and Fig. 7, there are variations in the centre frequencies between the simulated and fabricated antennas. The fabricated antenna has improved bandwidth in the lower

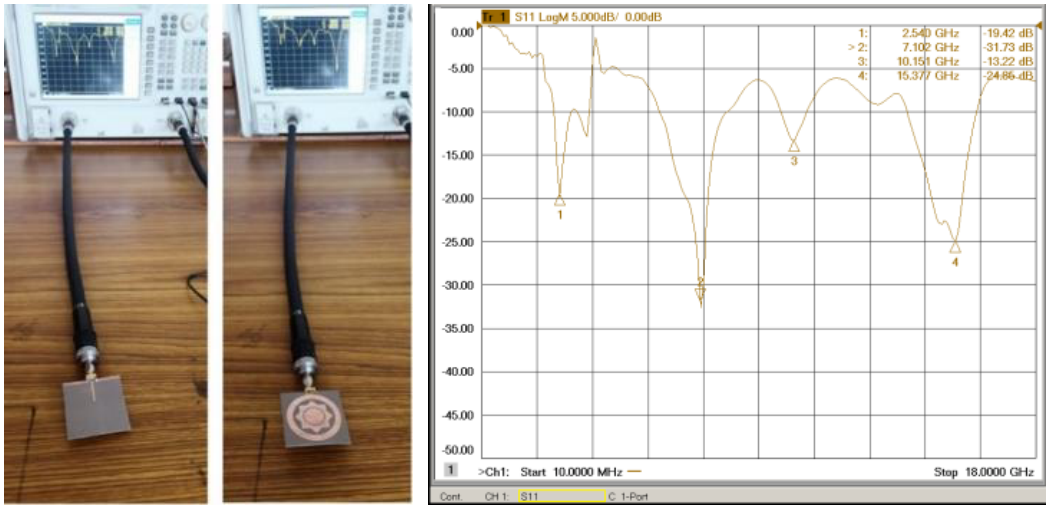

Figure 6. Measurement setup and results for S_{11} parameter of the fabricated antenna.

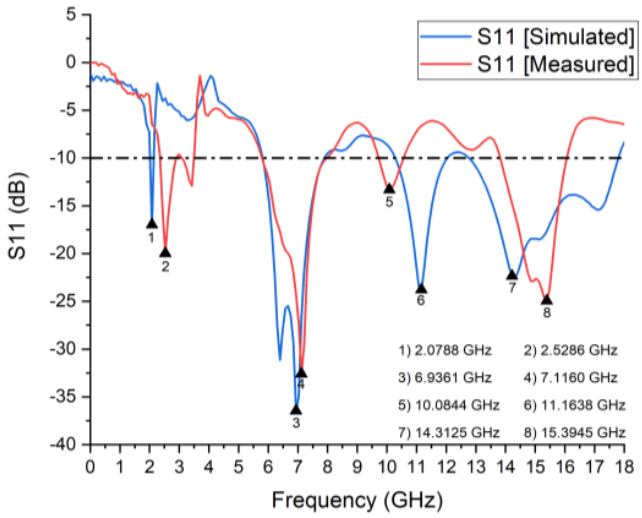

Figure 7. Simulated vs measured results for S_{11} for the proposed antenna.

frequency band and slightly decreased bandwidth in the upper frequency bands. The positive shift in frequency can be attributed to the fabrication tolerances and variations in the dielectric thickness. The SMA connector used in the fabricated design also has an impact on the high-frequency response as this is not modelled in simulation. Even with these variations the proposed design can be considered as a very good antenna for Wi-Fi applications in 2.4 GHz and 6 GHz band. Also, this can be considered for the use in VANET applications.

3.1. Equivalent Circuit Model

The antenna can be modelled as a coplanar waveguide fed rectangular patch antenna loaded with three parasitic patch resonators and defective ground plane. The equivalent circuit model is shown in Fig. 8, where Zf is the feed impedance; Zpr is the rectangular patch impedance; $Zgd1$ is the load on Zpr due to defective ground; $Zpar1$ is the impedance of parasitic outer annular ring patch; $Zgd1$ is the load on $Zpar1$ due to defective ground; $Zpar2$ is the impedance of parasitic middle annular ring patch. The defect on the annular ring is modelled as $Zpar2d$. $Zgd2$ is the defective ground load on $Zpar2$,

Table 2. Comparison of parameters of the simulated and measured values for the proposed antenna.

Parameter	Simulated	Measured
No. of Resonant Bands	4	4
Centre Frequency in GHz (S_{11} in dB)	a) 2.0880 [−17.224] b) 6.8555 [−29.797] c) 11.1635 [−23.786] d) 15.2925 [−18.115]	a) 2.6185 [−16.007] b) 6.8465 [−21.885] c) 10.1295 [−13.369] d) 14.9415 [−22.070]
Band Span in GHz	a) 2.043–2.133 b) 5.821–7.890 c) 10.300 – 12.027 d) 12.783–17.802	a) 2.349–2.888 b) 5.767–7.926 c) 9.725–10.534 d) 13.862 – 16.021
Bandwidth in GHz (% BW)	a) 0.09 (4.31) b) 2.069 (30.18) c) 1.727 (15.47) d) 4.299 (28.11)	a) 0.539 (20.58) b) 2.159 (31.53) c) 0.809 (7.98) d) 2.159 (14.45)

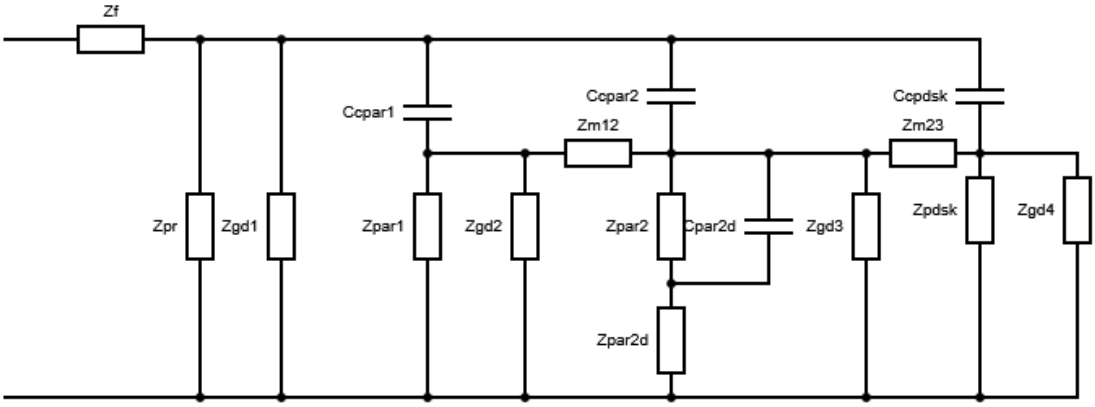

Figure 8. Equivalent circuit model of the antenna impedance from its structure.

and $Zpdsk$ is the impedance of the inner circular disk loaded with $Zgd4$ due to ground defect. $Zm12$ and $Zm23$ are mutual coupling impedances between the outer ring-middle ring and middle ring-inner disk, respectively. The values of these impedances can be computed using the equations available in [10, 13–18].

The antenna input impedance Zin is also modelled using the Foster representation where each radiating structure is modelled as a parallel RLC circuit [13]. The values for the RLC components are obtained from the electromagnetic (EM) simulation plot. LTSpice simulator is used to model the circuit, and its schematic is shown in Fig. 9. The S_{11} value obtained by simulation is given in Fig. 10 and is found to closely match with the CST simulated results.

3.2. Gain & Efficiency

The maximum gain over frequency is simulated and shown in Fig. 11. For the frequency range between 5.821 and 7.89 GHz, the gain varies between the minimum of 4.0185 dB and maximum of 6.3088 dB with an average value of 5.1637 dB. In the high frequency bands of 10.3-to-12.027 GHz and 12.783-to-17.802 the average simulated gains are 6.4779 dB and 6.9585 dB, respectively. The gain in the low frequency band of 2.043-to-2.133 GHz is less. For the fabricated antenna, the gain varies between a minimum of

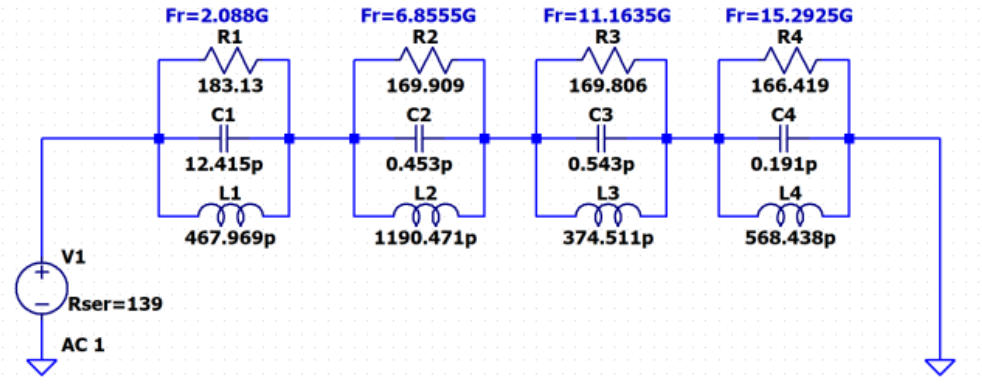

Figure 9. Equivalent circuit model using Foster approximation from EM simulated S_{11} values.

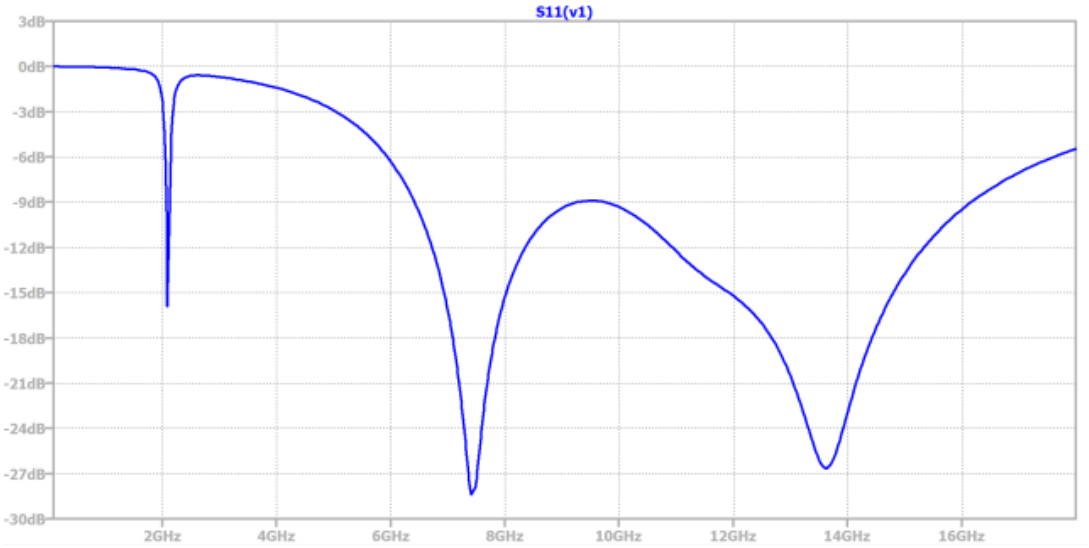

Figure 10. S_{11} results for the equivalent circuit model in Fig. 9.

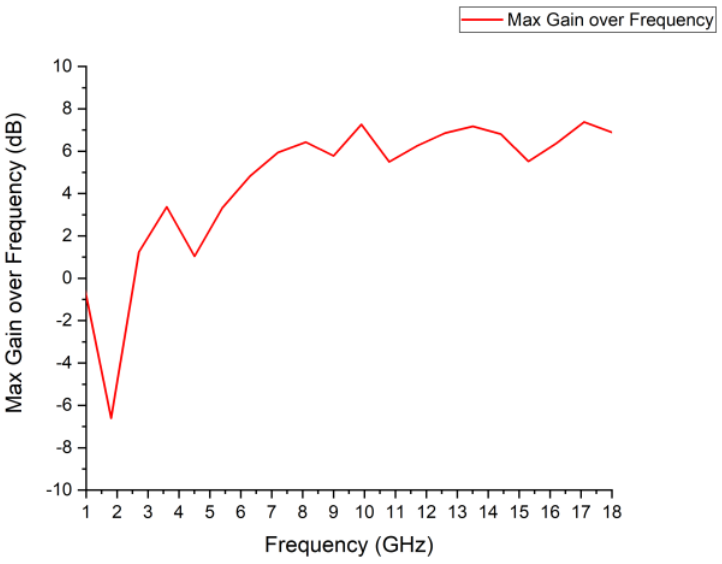

Figure 11. Simulation results for maximum gain over frequency.

3.75 dB and a maximum of 5.007 dB for the frequency range of 5.5-to-8 GHz, showing a good match between the simulated and measured results.

The simulated results for radiation and total efficiency of the proposed antenna are shown in Fig. 12. For the frequency range between 5.821 and 7.89 GHz, the total efficiency varies from −1.2954 dB to −0.4923 dB for frequencies 5.821-to-6.3212 GHz, beyond which the efficiency is almost constant with an average value of −0.64054 dB. For 10.3-to-12.027 GHz, the efficiency is almost constant with the average value −0.7655 dB. The efficiency is constant in the 12.783-to-17.802 GHz band with an average value of −0.79101 dB. Thus, the antenna has an efficiency of at least 83%. Thus, the simulated antenna can be considered as an efficient resonator at high frequencies.

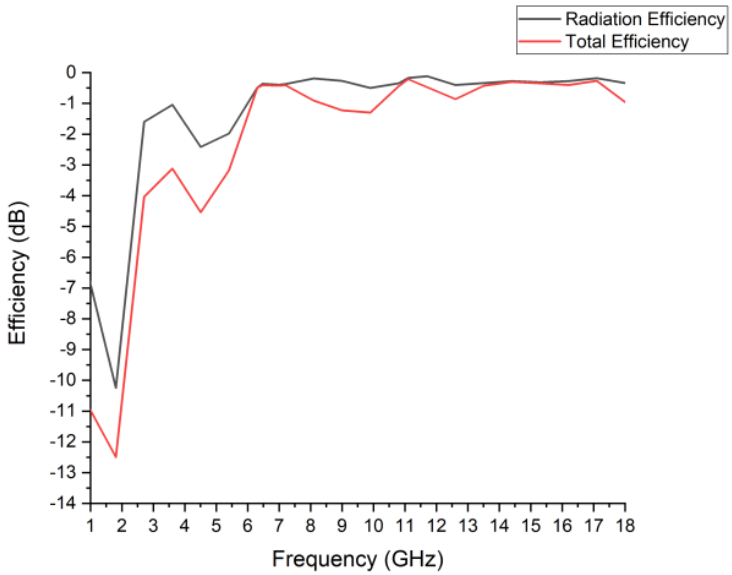

Figure 12. Simulation results for efficiency of the antenna.

3.3. Radiation Pattern

Radiation pattern of the fabricated antenna was measured in an anechoic chamber using a 50 Ω 1 GHz to 18 GHz broad Frequency Amkom Horn antenna as the transmitter. The measurement of radiation pattern was carried out by varying the angle in steps of 10 degrees for both E-plane and H-plane measurements at three frequencies of 6.475 GHz, 7 GHz, and 11.1 GHz. The measured results are compared with the simulated ones at the same frequencies, and the plots are given in Fig. 13.

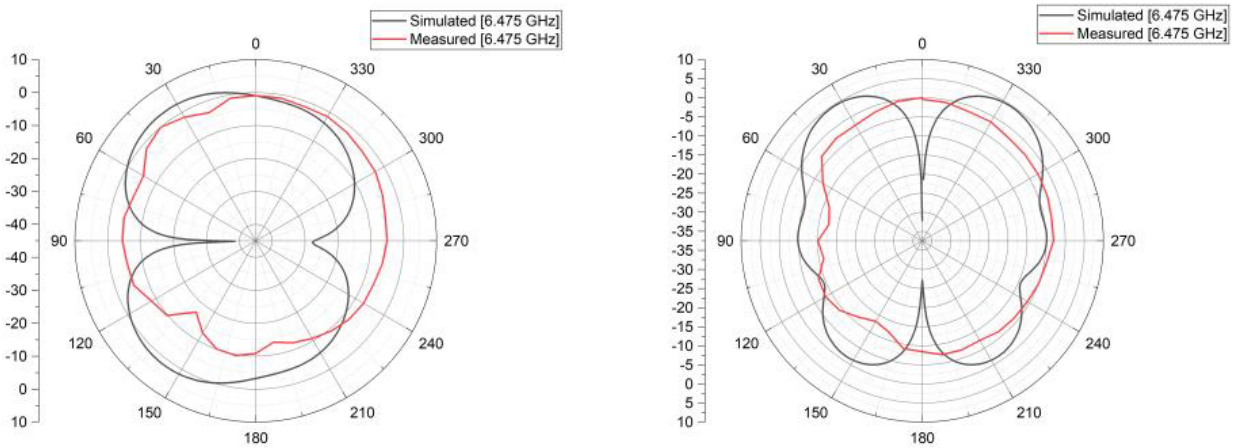

(a) (b)

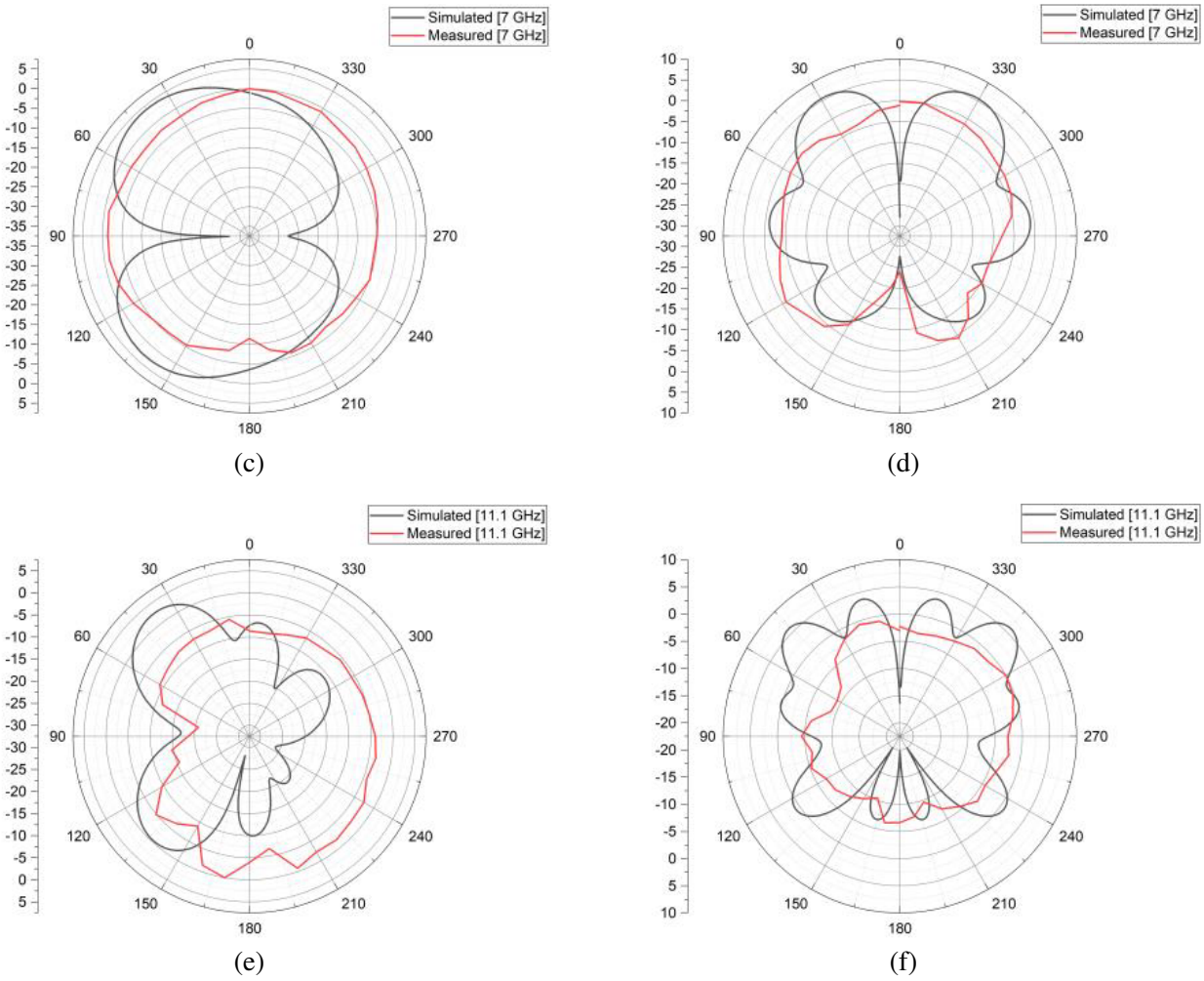

Figure 13. *E*-plane & *H*-plane radiation patterns of the proposed antenna at 6.475 GHz, 7 GHz, and 11.1 GHz. (a) *E*-plane at 6.475 GHz, (b) *H*-plane at 6.475 GHz, (c) *E*-plane at 7 GHz, (d) *H*-plane at 7 GHz, (e) *E*-plane at 11.1 GHz, (f) *H*-plane at 11.1 GHz.

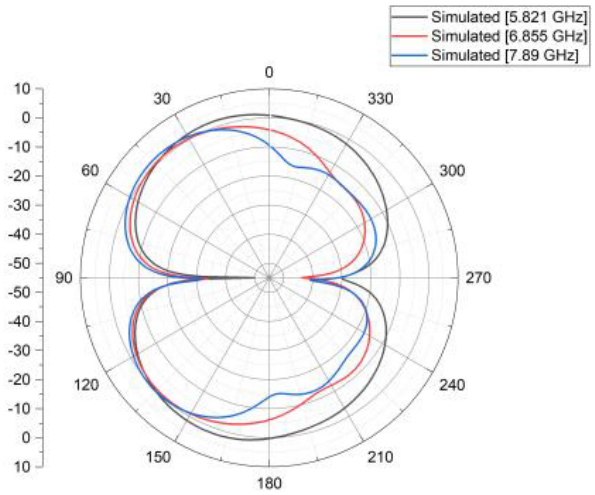

Figure 14. Radiation pattern variation in *E*-plane for 5.821-to-7.890 GHz.

The variation of E-plane radiation pattern at different frequencies in the 6 GHz band is shown in Fig. 14. At 5.821 GHz, the main lobe direction is 21 degrees with the angular width of 72.6 degrees. At 6.855 GHz, the angular width of 55.4 degrees is obtained with the main lobe direction at 39 degrees. At 7.890 GHz, the main lobe shifts to 43 degrees with an angular width of 47.3 degrees. Considering the entire 5.821-to-7.890 GHz frequency range, the antenna radiation is between 19.35 and 57.3 degrees with an angular width of 37.95 degrees.

3.4. Current Distribution

The current distribution in the proposed antenna is shown in Fig. 15. There are 4 currents in the patch. The first one is in the coplanar fed monopole antenna, second in the outer annular ring, third in annular star patch, and fourth in the central disk. These currents give rise to the four resonant bands. Maximum currents of 148.691 A/m at 2.088 GHz, 32.2835 A/m at 6.8555 GHz, 33.3452 A/m at 11.1635 GHz, and 30.3942 A/m at 15.925 GHz are observed. The low current is due to the parasitic nature of the antenna. Hence this antenna can be considered for low-power applications.

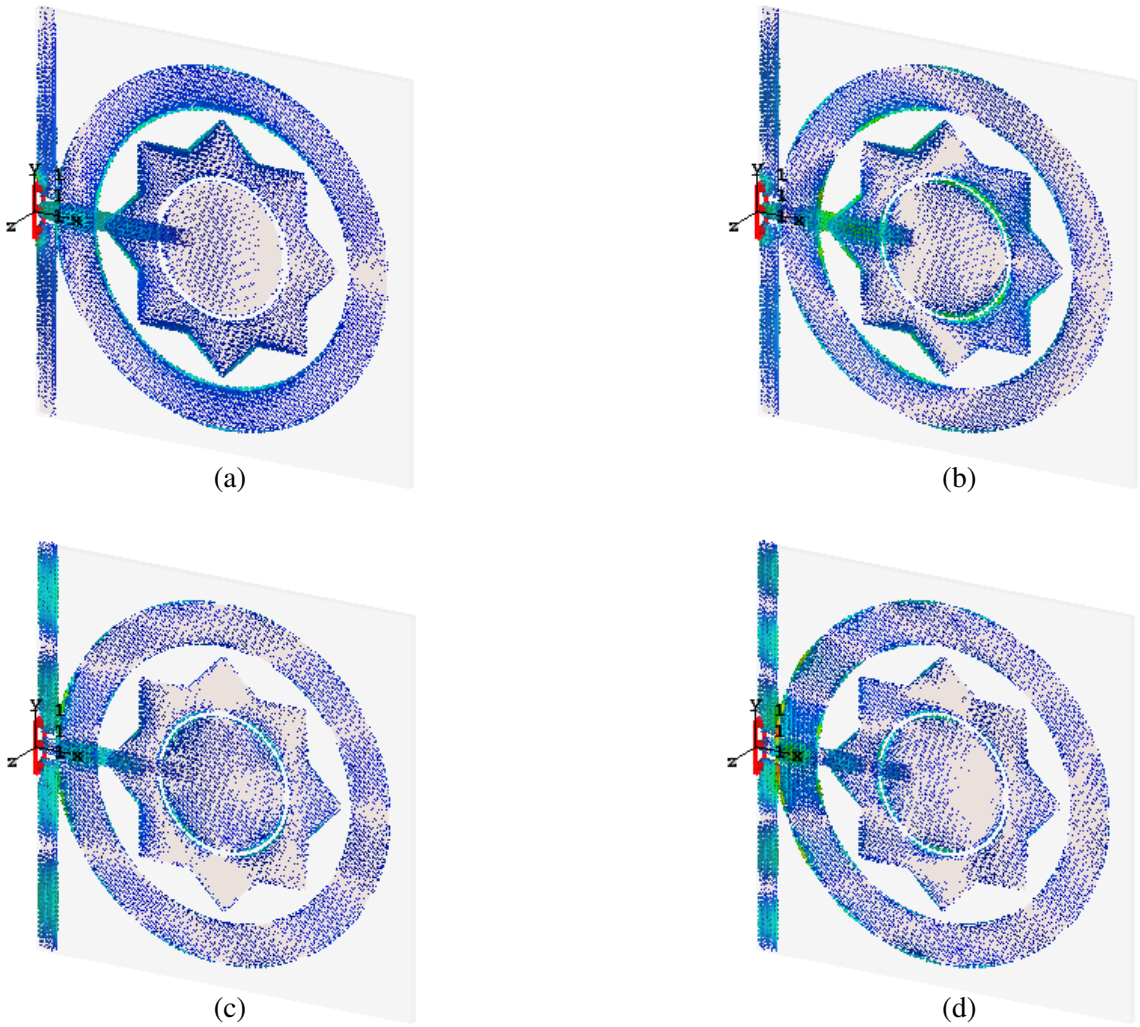

Figure 15. Surface current distribution of the proposed antenna at different centre frequencies. (a) 2.088 GHz, (b) 6.8555 GHz, (c) 11.1635 GHz, (d) 15.2925 GHz.

3.5. Comparative Study

The proposed antenna is compared with currently available 6 GHz antennas and summarized in Table 3. It can be seen that the proposed antenna supports quad bands of 2.088/6.97/11.13/14.29 GHz. In addition, it has a moderate size and better gain characteristics.

Table 3. Comparative summary of the proposed antenna with available 6 GHz antennas.

Antenna	Antenna Parameters				
	Size (mm^3)	**Center Frequency (GHz)**	**Bandwidth (GHz)**	**Max Gain (dB)**	**Efficiency (%)**
Maddio et al. [19]	$65 \times 65 \times 1.6$	2.45, 5.1	NA	5.9, 6.15	NA
V. R. Kanni et al. [20]	$20.2 \times 24.1 \times 1.6$	5.9	0.075	5.6	78
Singhal et al. [21]	Hexagonal $\pi \times 20 \times 1.6$	5.9	0.2	5.9	NA
Maddio et al. [22]	$25 \times 48 \times 1.6$	5.81	0.5	7.12	NA
D. S. Woo [23]	$28 \times 24 \times 1$	2.4, 3.5, 5.9	0.21, 0.3, 0.5	2.3, 2.6, 3.7	NA
This Work Antenna_5	$50 \times 50 \times 1$	2.088, 6.97, 11.13, 14.29	0.09, 2.069, 1.722, 4.299	6.47	83

4. CONCLUSION

The article details the design and simulation results of five coplanar fed parasitic microstrip patch antenna structures for the use in wireless applications. One of the proposed designs (Antenna_5) is fabricated, experimented, and results are presented. The proposed antenna has radiating dimension of 50 mm × 50 mm × 1 mm and resonates in four different bands, 2.02–2.14 GHz [Band-A], 5.81–7.89 GHz [Band-B], 10.28–12.04 GHz [Band-C], and 12.79–17.8 GHz [Band-D] with resonant peaks at 2.088 GHz, 6.97 GHz, 11.13 GHz, and 14.29 GHz, respectively. Equivalent circuit model for the proposed antenna is also given. Antenna characteristics observed at 5.81–7.89 GHz band have shown excellent radiation pattern for 6 GHz wireless applications. The measured results were in close conformity with the simulated ones.

REFERENCES

1. Marcus, M. and B. Pattan, "Millimeter wave propagation: Spectrum management implications," *IEEE Microwave Magazine*, Vol. 6, No. 2, 54–62, Jun. 2005, doi: 10.1109/mmw.2005.1491267.
2. GSM Association, "The 6 GHz ecosystem: Demand drives scale," Aug. 2022. Accessed: Jan. 17, 2023. [Online]. Available: https://www.gsma.com/spectrum/wp-content/uploads/2022/08/6-GHz-IMT-Ecosystem.pdf.
3. Ansari, J. A., K. Kumari, A. Singh, and A. Mishra, "Ultra-wideband co-planer microstrip patch antenna for wireless applications," *Wireless Personal Communications*, Vol. 69, No. 4, 1365–1378, May 2012, doi: 10.1007/s11277-012-0638-y.
4. Bakariya, P. S., S. Dwari, M. Sarkar, and M. K. Mandal, "Proximity-coupled multiband microstrip antenna for wireless applications," *IEEE Antennas and Wireless Propagation Letters*, Vol. 14, 646–649, 2015, doi: 10.1109/lawp.2014.2376693.
5. Ketavath, K. N., "Enhancement of gain with coplanar concentric ring patch antenna," *Wireless Personal Communications*, Vol. 108, No. 3, 1447–1457, May 2019, doi: 10.1007/s11277-019-06478-9.

6. Kanaujia, B. K. and B. R. Vishvakarma, "Design considerations for the development of the annular ring microstrip antenna," *International Journal of Electronics*, Vol. 89, No. 8, 665–677, Aug. 2002, doi: 10.1080/00207210210005752 6.
7. Singh, A. K., R. K. Gangwar, and B. K. Kanaujia, "Circularly polarized annular ring microstrip antenna for high gain application," *Electromagnetics*, Vol. 36, No. 6, 379–391, Aug. 2016, doi: 10.1080/02726343.2016.1207801.
8. Kumar, G. and K. P. Ray, *Broadband Microstrip Antennas*, Artech House, Deedham, MA, USA, 2002.
9. Bahl, I. J. and P. Bhartia, *Microstrip Antennas*, Artech House, Dedham, MA, USA, 1980.
10. Simons, R. N., *Coplanar Waveguide Circuits, Components, and Systems*, Vol. 152, Wiley-IEEE Press, 2002, doi: 10.1604/978047122475410.1002/0471224758.
11. Balanis, C. A., *Antenna Theory: Analysis and Design*, 4th Edition, Wiley, 2016.
12. Terman, F. E., *Electronic and Radio Engineering*, McGraw-Hill Book Company, Inc., USA, 2003, doi: 10.1604/9780758184740.
13. Singh, A., K. Shet, D. Prasad, A. K. Pandey, and M. Aneesh, "A review: Circuit theory of microstrip antennas for dual-, multi-, and ultra-widebands," *Modulation in Electronics and Telecommunications*, Mar. 2020, doi: 10.5772/intechopen.91365.
14. Singh, A., J. A. Ansari, Kamakshi, M. Aneesh, and S. S. Sayeed, "L-strip proximity fed gap coupled compact semi-circular disk patch antenna," *Alexandria Engineering Journal*, Vol. 53, No. 1, 61–67, Mar. 2014, doi: 10.1016/j.aej.2013.12.001.
15. Singh, A., M. Aneesh, and J. A. Ansari, "Analysis of microstrip line fed patch antenna for wireless communications," *Open Engineering*, Vol. 7, No. 1, 279–286, Nov. 2017, doi: 10.1515/eng-2017-0034.
16. Ez-Zaki, F., K. A. Belaid, S. Ahmad, et al., "Circuit modelling of broadband antenna using vector fitting and foster form approaches for IoT applications," *Electronics*, Vol. 11, No. 22, 3724, Nov. 2022, doi: 10.3390/electronics11223724.
17. Shen, L. C., "Analysis of a circular-disc printed-circuit antenna," *Proceedings of the Institution of Electrical Engineers*, Vol. 126, No. 12, 1220, 1979, doi: 10.1049/piee.1979.0210.
18. Bhattacharyya, A. and R. Garg, "Input impedance of annular ring microstrip antenna using circuit theory approach," *IEEE Transactions on Antennas and Propagation*, Vol. 33, No. 4, 369–374, Apr. 1985, doi: 10.1109/tap.1985.1143584.
19. Maddio, S., G. Pelosi, M. Righini, and S. Selleri, "A circularly polarized antenna for dual band operation at 2.45 GHz and 5.10 GHz," *Progress In Electromagnetics Research C*, Vol. 74, 1–8, 2017.
20. Renuga Kanni, V. and R. Brinda, "Design of high gain microstrip antenna for vehicle to vehicle communication using genetic algorithm," *Progress In Electromagnetics Research M*, Vol. 81, 167–179, 2019.
21. Singhal, H., S. Ashwin, V. Sharma, J. Prajapati, and M. D. Upadhayay, "High gain hexagonal patch antenna for V2V communication," *2020 7th International Conference on Signal Processing and Integrated Networks (SPIN)*, 687–691, Noida, India, 2020, doi: 10.1109/SPIN48934.2020.9071270.
22. Maddio, S., G. Pelosi, M. Righini, and S. Selleri, "A slotted patch antenna with enhanced gain pattern for automotive applications," *Progress In Electromagnetics Research Letters*, Vol. 95, 135–141, 2021.
23. Woo, D. S., "A triple band C-shape monopole antenna for vehicle communication application," *Progress In Electromagnetics Research C*, Vol. 121, 97–106, 2022.